
1 When the MOUSE leaves the house

2 Bernhard Blümich¹, Jens Anders²

3 ¹Institut für Technische und Makromolekulare Chemie, RWTH Aachen University, 52159 Roetgen, Germany,

4 ²Institute of Smart Sensors, University of Stuttgart, 70569 Stuttgart, Germany

5 Correspondence to: Bernhard Blümich (bluemich@rwth-aachen.de)

6 **Abstract.** Change is inherent to time being transient. With the NMR-MOUSE having matured into an established
7 NMR tool for non-destructive testing of materials, this forward-looking retrospective assesses the challenges the
8 NMR-MOUSE faced when deployed outside a protected laboratory and how its performance quality can be
9 maintained and improved when operated under adverse conditions in foreign environments. This work is dedicated
10 to my dear colleague and friend Geoffrey Bodenhausen on the occasion of his crossing an honorable timeline in
11 appreciation of his ever-continuing success of fueling the dynamics of magnetic resonance.

12 1. Introduction

13 The MOUSE (MOBile Universal Surface Explorer) (Eidmann et al., 1996) is a portable stray-field NMR sensor
14 suited for non-destructive testing of materials (Blümich et al., 2008; Casanova et al., 2011) With it the relaxation
15 of nuclear spins towards equilibrium is measured following perturbation by radio-frequency pulses. The sensor is
16 a small and compact NMR relaxometer that investigates an object from one side and can be carried along to the
17 site of interest. As such the NMR-MOUSE and other stray field relaxometers are one modality of compact NMR.
18 Other modalities are tabletop relaxometers, tabletop imagers and tabletop spectrometers (Blümich et al., 2014;
19 Blümich, 2016; Blümich and Singh, 2018).

20 While the size of most NMR instruments today is dominated by a large superconducting magnet, compact
21 NMR relaxometers have small permanent magnets. They were commercially introduced in the early 1970ies to
22 assist the food industry in characterizing emulsions (van Putte and van den Enden, 1974; Blümich, 2019). Today
23 tabletop relaxometers are employed to study a wide range of materials, in particular, foodstuffs, polymers, and
24 porous media (Blümich et al., 2014; Blümich, 2016; Blümich and Singh, 2018; Saalwächter, 2012). A key feature
25 of these early tabletop instruments is that samples need to be drawn and inserted into the hole in the magnet for
26 analysis. In this respect, the measurement is destructive. This equally applies to modern tabletop NMR
27 spectrometers for chemical analysis unless they are operated in flow-through mode, like in a process control
28 environment (Kern et al., 2019). While NMR spectrometers with permanent magnets were built already in the
29 early 1950s (Gutowski, 1953; Blümich, 2019), their magnets were large and could produce only a small field
30 region sufficiently homogeneous to resolve the proton chemical shift. Small permanent magnets with
31 homogeneous fields are challenging to build due to the variations in dimensions, polarization magnitude, and
32 direction of the magnet elements. Therefore, the routine use of compact NMR instruments remained limited for a
33 long time to relaxation and diffusion measurements until the technology of compact high-resolution magnets had
34 been sufficiently advanced about ten years ago (Danieli et al., 2010; Blümich, 2016; Blümich and Singh, 2018).
35 Before that, chemical analysis with tabletop instruments was explored primarily by a few dedicated research
36 groups (Nordon et al., 2001; Dalitz et al., 2012).

hat formatiert: Deutsch

hat gelöst: ¹Independent researcher, 52159 Roetgen, Germany

39 Mobile NMR instruments need to be both compact and robust to deploy them at different sites and in
40 different environments. The era of mobile NMR began with well-logging instruments shortly after the first NMR
41 experiments in condensed matter in December 1945. Already in 1952, Russel Varian patented a subsurface well
42 logging method and apparatus (Varian, 1952; Woessner, 2001). The sensor to be inserted into the borehole of an
43 oil-well and operating in the earth's magnetic field eventually evolved into tube-shaped instruments housing
44 permanent magnets as well as transmit and receive electronics to analyze the relaxation of ^1H NMR signals from
45 particular regions localized in the borehole wall (Jackson et al., 1980; Kleinberg and Jackson, 2001). In his
46 introduction to the 2016 book "Mobile NMR and MRI" (Johns et al., 2016), Eiichi Fukushima reviews the
47 evolution of earth-field and mobile NMR with particular attention to these early developments (Fukushima, 2016).

48 Well-logging NMR is also known as inside-out NMR because the instrument is inserted into the object and
49 not the object into the magnet. Inside-out NMR is mobile but also destructive, as a hole needs to be drilled into the
50 object (Jackson et al., 1980; Coates et al., 1999). The underlying concept of mobile stray-field relaxometry was
51 extended at the Southwest Research Institute, San Antonio, Texas, to nondestructive materials testing with NMR
52 relaxometers accessing the object from one side. These instruments were already transportable, whereby some of
53 them using bulky and massive electromagnets, others more compact permanent magnets (Fukushima, 2016). The
54 magnets were laid out to maximize the field volume containing the spins which can be excited selectively from
55 within the bulk with rf pulses in an effort to maximize the hydrogen signal from the object of interest next to the
56 sensor deriving from moisture in soil, bridge decks, building structures, and food products (Fukushima, 2016;
57 Blümich et al., 2008; Blümich, 2016; Blümich, 2019). Within this volume the field gradient must be small so that
58 the resonance frequencies of the spins inside are within the bandwidth of the rf excitation pulses. As a consequence,
59 the field strength was low.

60 One may argue that the era of mobile NMR with compact sensors essentially started with the appearance
61 of the NMR-MOUSE, a stray-field relaxometer that in its design disregarded the quest for a large sensitive volume
62 by fortuitous ignorance (Eidmann et al., 1996). The small sensor exhibits a large field gradient, and consequently
63 a small sensitive volume yet a strong stray field. Compared to larger sensors the opposing impacts on the sensitivity
64 of a smaller signal-bearing volume and higher field strength turned out to largely balance each other so that at
65 comparable sensitivity the more compact sensors (Blümich et al., 2008) were easier to carry along and be moved
66 from one place to another than other stray-field sensors.

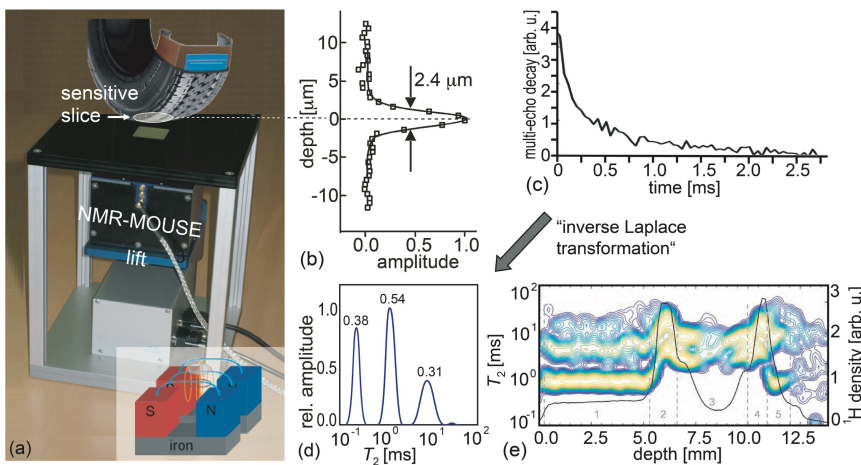
67 2. The NMR-MOUSE in the house

68 While brainstorming the simplest realization of NMR in 1993 at the Max-Planck Institute for Polymer Research
69 in Mainz, Peter Blümmler asked the question: "Would it not be nice to have an NMR scanner that one moves across
70 the surface of an object to look inside just like an ultrasound scanner?" (Armstrong-Smith, 2015). The next day he
71 came with a drawing how such a device could look like, and we dubbed it NMR-MOUSE for 'MOBILE Universal
72 Surface Explorer'. Having taken up the Chair of Macromolecular Chemistry at RWTH Aachen University the
73 same year, the realization of the NMR-MOUSE was the project of Blümich's first PhD student Gunnar Eidmann,
74 who succeeded to get the first signal in 1995 (Eidmann et al., 1996). Hardware improvements, measurement
75 methodology and applications of the NMR-MOUSE were systematically explored over the years in particular by
76 Peter Blümmler, Gisela Guthausen, Sophia Anferova, Valdimir Anferov, Federico Casanova and Juan Perlo. The
77 NMR-MOUSE has found numerous applications for nondestructive materials characterization by relaxation and

78 diffusion measurements (Blümich et al., 2008; Casanova et al., 2011). The design of many early stray-field
 79 relaxometers and of the original NMR-MOUSE was that of a simple u-shaped magnet. It is marketed by Bruker
 80 under the name ‘minispec Profiler’. This sensor has a roughly cup-shaped sensitive volume, the position, and
 81 shape of which are defined by the profiles of the stray fields produced by the permanent magnet and the radio-
 82 frequency coil (Eidmann et al., 1996, Hürlimann and Griffin, 2000; Balibanu et al., 2000).

83 A major improvement of the original sensor was to shim the sensitive volume from bowl-shape to a flat
 84 with a slice diameter of about 10 mm, and, depending on the measurement scheme, a slice width less than 3 μm
 85 (Perlo et al., 2005), enabling the acquisition of high-resolution depth profiles by translating the sensor in-between
 86 measurements with high precision. To this end, two u-shaped or horseshoe magnets are placed side by side with a
 87 small gap (Fig. 1a, bottom). The measurement principle followed to acquire depth profiles is the same as that
 88 employed for logging oil wells except that the NMR-MOUSE sensor is horizontally moved between consecutive
 89 measurements in steps on the order of 0.1 mm instead acquiring NMR signal while the well-logging tool is moving
 90 laterally with respect to the magnet surface for distances on the order meters. Today, the NMR-MOUSE for high-
 91 resolution depth profiling is a heritage product of Magritek GmbH with its production site in Aachen, that is
 92 managed by the two NMR-MOUSE pioneers Federico Casanova and Juan Perlo. In fact, Magritek today is the
 93 result of a 2012 merger of Magritek Ltd. from New Zealand, which, among others, developed the Kea spectrometer
 94 motivated by Paul Callaghan’s Antarctic expeditions (Callaghan et al., 1998), and ACT GmbH, a company spun
 95 off from RWTH Aachen University, which produced the Profile NMR-MOUSE.

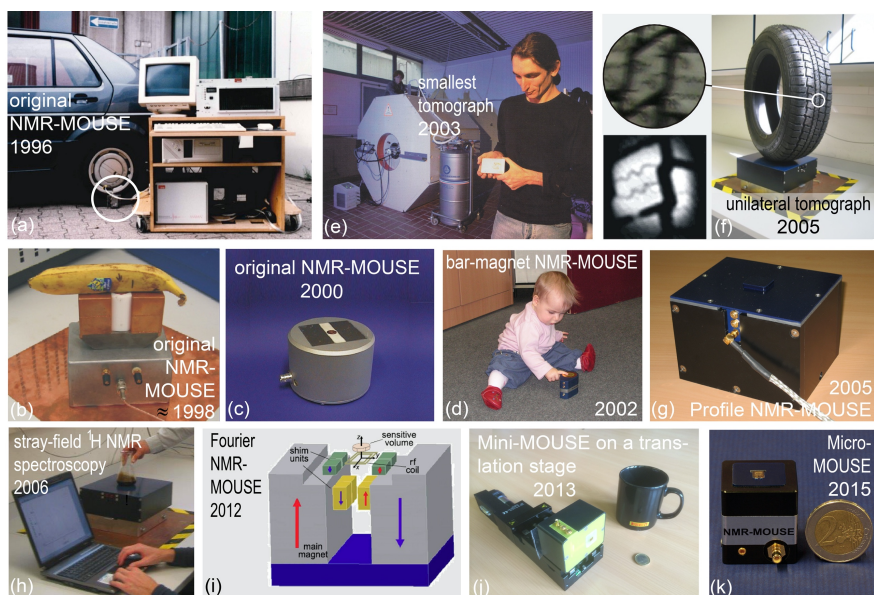
96



97
 98 Figure 1. The principle of measuring depth profiles with the Profile NMR-MOUSE. a) Conceptual picture of the
 99 profile NMR-MOUSE on a lift with its sensitive slice inside a rubber tire. b) Point-spread function of the record
 100 depth resolution. c) Experimental signal decay measured with a multi-echo train. d) Distribution of relaxation
 101 times from tire-tread rubber derived by inversion of a signal decay with an algorithm, referred to as “inverse
 102 Laplace transformation”. e) Collection of distributions of relaxation times and signal amplitudes reporting nominal
 103 spin density measured across a range of 14 mm into a tire tread.
 104

105 To measure depth profiles, the sensor is mounted on a precision displacement stage with which the sensitive
 106 slice at a fixed distance from the magnet surface can be moved through the object step by step between acquisitions
 107 of multi-echo trains and more advanced two-dimensional Laplace methods (Blümich et al., 2014). The envelope

108 of a multi-echo train provides a stroboscopically sampled transverse relaxation decay (Fig. 1c) from which a depth-
 109 profile amplitude can be derived in different ways to provide NMR parameter contrast based the relaxation-time
 110 distribution (Fig. 1d), the hydrogen density corresponding to the signal amplitude from the spins in the sensitive
 111 slice (Fig. 1e), relaxation times, and molecular self-diffusion (Blümich et al., 2008; Casanova et al., 2011; Blümich
 112 et al., 2014). The signal amplitude is the full integral of the relaxation-time distribution. Partial integrals of
 113 individual peaks provide component concentrations. To assign physical meaning to individual peaks is not as
 114 straight forward as interpreting the chemical shift of resonance lines in a high-resolution NMR spectrum. Yet the
 115 peak amplitudes and positions vary with material properties (Fig. 1e), and it often takes the treasure of experience
 116 or a reference data base to interpret distributions of relaxation times for practical applications.
 117



118
 119 Figure 2. The evolution of stray-field NMR at RWTH Aachen University. a) The original NMR-MOUSE
 120 measuring a car tire. b) An early version of the NMR-MOUSE with copper-shielded magnets for dead-time
 121 reduction. c) The original NMR-MOUSE in 2000. d) The bar-magnet NMR-MOUSE is the simplest construction
 122 of a stray-field NMR sensor. e) In 2003 Juan Perlo developed the smallest tomograph in stray-field technology
 123 (Foto: Peter Winandy). f) A single-sided tomograph with a flat imaging plane. Right: Set-up for mapping a tire
 124 tread. Left: A photo (top) in comparison with an MR image (bottom). g) The Profile NMR-MOUSE with a flat
 125 sensitive slice developed in 2005. h) Stray-field NMR magnet capable of measuring chemical-shift resolved ¹H
 126 NMR spectra from a fluid in a beaker placed on top of the magnet. i) Fourier NMR-MOUSE with shim magnets
 127 producing a 2 mm thick sensitive slice for frequency encoding of depth. j) Mini-MOUSE with a multi-layered
 128 micro-coil having a dead-time of 10 μs. k) Micro-MOUSE constructed from four 1 cm³ permanent magnet cubes.
 129

130 The hardware, use, and measurement methodology of the NMR-MOUSE has been studied for more than
 131 two decades in various research projects at RWTH Aachen University and other places. Its use for testing different
 132 materials such as rubber, polymers, building materials, food, and objects of cultural heritage is reported in books
 133 and reviews (Blümich, 2000; Blümich, 2008; Blümich et al., 2008; Blümich et al., 2010; Casanova et al., 2011;
 134 Capitani et al., 2012; Blümich et al., 2014, Baías and Blümich, 2017; Capitani et al., 2017, Blümich, 2019; Rehorn
 135 and Blümich, 2018; Blümich, 2019). Several modifications of the original NMR-MOUSE in addition to the

136 forerunner of the current Magritek Profile NMR-MOUSE (Fig. 1a) have been investigated at RWTH Aachen
137 University. Recognizing that the information content extractable from the signal of the sensitive region in stray-
138 field NMR corresponds to that accessible in a voxel of a magnetic resonance image, first applications of the NMR-
139 MOUSE were explored with car tires representing soft synthetic matter (Fig. 2a) in line with the main use of MRI
140 in imaging soft biological matter. The horseshoe set-up (Fig. 2b) was subsequently made smaller and packed in a
141 more attractive shell (Fig. 2c). Realizing that the horse-shoe magnet having the B_0 stray field essentially parallel
142 to its active surface could further be simplified, the bar-magnet NMR-MOUSE was built from a magnet block first
143 cuboid-shaped (Blümich et al., 2002) and later cylinder-shaped with B_0 perpendicular to the active end face and a
144 figure-eight rf coil with B_1 parallel to it (Fig. 2d). The maximum depth of access is lower than for the horseshoe
145 sensor, but the deadtime is shorter due to the gradiometer property of the rf coil (Anferova et al., 2002). Note that
146 contrary to the B_0 orientation perpendicular to the active surface, B_0 parallel to the active surface enables studying
147 macroscopic molecular order in anisotropic materials such as tendon and strained rubber (Haken and Blümich,
148 2000; Hailu et al., 2002).

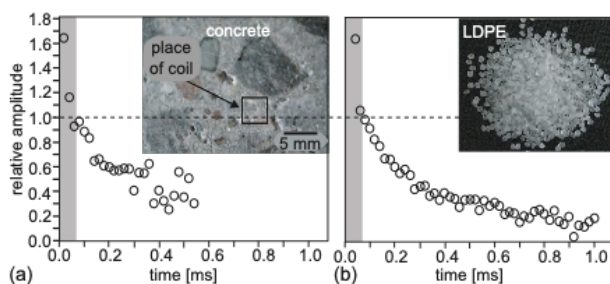
149 While improving the original NMR-MOUSE, also a single-sided tomograph was developed and tested in
150 the DFG-funded Collaborative Research Center on Surface NMR of Elastomers and Biological Tissue FOR333.
151 One result from this project was the smallest MRI instrument at the time obtained by fitting a bar-magnet NMR-
152 MOUSE with coils for pulsed gradient fields (Fig. 2e) (Casanova and Blümich, 2003). Another result was an
153 improved u-shaped magnet with thicker ends at each side of the poles so that the magnet assembly produced a flat
154 imaging plane (Fig. 2f) (Casanova and Blümich, 2003; Blümich et al., 2005). Images from a plane parallel to the
155 sensor surface could be measured with pure phase encoding schemes, but the sensitivity was low due to the thin
156 slice resulting from a strong stray-field gradient. Maintaining the flat sensitive region of the imaging plane, this
157 complex magnet geometry was subsequently simplified to two u-shaped magnets placed at a specific distance next
158 to each other, resulting in the Profile NMR-MOUSE (Fig. 1a, Fig. 2g), which proved to be a robust stray-field
159 NMR sensor constructed from a minimum number of parts (Perlo et al., 2005).

160 Flattening the sensitive region of a stray-field magnet to a plane was a milestone in understanding how to
161 shim the stray field. Eventually, the sensitive region in the stray field could be homogenized locally with the help
162 of additional shim magnets to a degree sufficient to resolve the ^1H chemical shift from a limited volume of fluid
163 inside a beaker on top of the magnet (Fig. 2h) (2014; Perlo et al., 2005; Perlo et al., 2006; Zalesskiy et al.). Another
164 advance was the construction of a stray-field sensor with a sensitive slice having a homogeneous gradient field in
165 the sensitive slice across an extended depth range of 2 mm for single-shot depth profiling by frequency encoding
166 of position (Fig. 2i) (Van Landeghem et al., 2012). With this sensor the time to acquire a depth profile into soft
167 matter was reduced considerably, and it proved useful for *in vivo* applications like mapping human skin [46] and
168 monitoring perfusion states of the small intestine by diffusion maps (Krechenau et al., 2018).

169 The NMR-MOUSE has also been miniaturized and fitted with multi-layered micro-coils (Fig. 2j,k)
170 (Oligschläger et al., 2014; Oligschläger, Kupferschläger, et al. 2015), by which, on the expense of 7.6-fold lower
171 sensitivity compared to the PM5 NMR-MOUSE at 1 mm access depth, the dead time of the measurement could
172 be reduced to a record 10 μs echo time. With its small coil, the signal from the cement regions between the stone
173 aggregate in cuts of concrete could be focused on, and with an echo time $\leq 20 \mu\text{s}$ the hitherto hidden signals from
174 bound water in the dry grey cement could be measured (Fig. 3a) (Oligschläger, Kupferschläger, et al. 2015). At
175 the same echo time, even the rapidly relaxing transverse magnetization from the crystalline domains of
176 polyethylene was detectable (Fig. 3b). The presence of the rapidly decaying signal components at $t_E = 20 \mu\text{s}$ nearly

177 doubles the amplitude of the recorded magnetization decays compared to the amplitudes recorded with the
 178 minimum echo time of 70 μs of the reference laboratory NMR-MOUSE with 10 mm depth of access. As the short
 179 dead time of the mini-MOUSE had been achieved at the cost of a small sensitive volume and a low depth of access
 180 due to the small diameter of the coil, it is the ambition of current sensor improvement to reduce the deadtime at
 181 coil diameters 10 mm and more. Currently, for example, the minimum echo time of the Magritek PM25 NMR-
 182 MOUSE is 50 μs when fitted with spacers and a 15 mm diameter coil to limit the depth of access to 10 mm. For a
 183 new PM2 NMR-MOUSE with 2 mm depth of access the minimum echo time of the is just 15 μs . Even shorter
 184 echo times may eventually be realized with novel transceiver circuits that promise the detection of the spin
 185 response during the rf pulse (Anders, 2020). Moreover, to shorten the acquisition time from hours to minutes for
 186 field applications like investigations of glass- or carbon-fiber reinforced polymer materials employed in windmill
 187 wings and airplane rudders, the detection of the bitumen component in asphalt (Blümich et al., 2019) and the bound
 188 water in cement, a large sensitive volume is needed. This can be achieved, for example, with a coil array
 189 (Oligschläger, Lehmkuhl, et al. 2015) [53] placed on a suitably tailored magnet surface (Blümich et al., 1999).

190



191

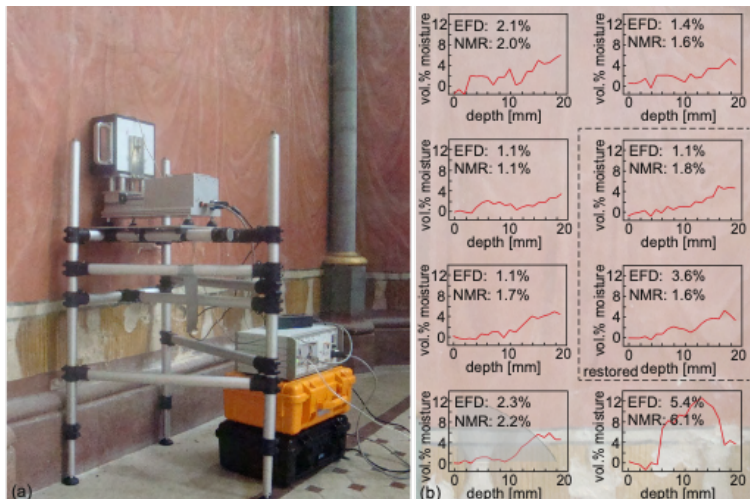
192 Figure 3. Transverse magnetization decays acquired with the Mini-MOUSE (Fig. 2j) at short echo time t_E . The
 193 shaded area marks signal lost at a deadtime of 70 μs . a) The signal from bound water in dry, grey cement. b) The
 194 crystalline protons in low-density polyethylene with $T_2 = 12 \mu\text{s}$ can be detected at $t_E = 20 \mu\text{s}$.

195 3. The NMR-MOUSE outside the house

196 The NMR-MOUSE was introduced to the cultural heritage community through the effort of Annalaura Segre at
 197 the turn of the millennium (Segre and Blümich, 2002), and from 1999 to 2019 its further refinement has benefitted
 198 greatly from the cultural heritage projects EUREKA-Eurocare Σ 12212-MOUSE, EU-ARTECH, CHARISMA, and
 199 IPERION-CH. With the exception of well-logging relaxometry (Coates et al, 1999), it is common practice to
 200 conduct NMR measurements in a laboratory. But objects of cultural heritage often cannot leave the museum or
 201 are immobilized, e. g. at excavation sites, so that the NMR-MOUSE has to be moved to the site and operated under
 202 the prevailing environmental and climatic conditions. These can be rather challenging at times for the operators as
 203 well as for the equipment, which has been designed primarily for indoor use.

204 For some outdoor applications like determining the crumb-rubber content in asphalt pavements (Blümich
 205 et al., 2019), depth profiling is not essential. But for others it is crucial. This includes the analysis of easel paintings
 206 (Presciutti et al., 2008; Fife et al., 2015; Angelova et al., 2016; Prati et al., 2019; Busse et al., 2020), frescoes
 207 (Rehorn et al., 2018), and mummies (Rühli et al., 2007; Blümich et al., 2014). A less obvious application is the
 208 analysis of moisture distributions, for example, in walls. Moisture maps with crude lateral resolution and high

209 depth resolution can assist in locating a moisture leak (Proietti et al., 2007; Rehorn and Blümich, 2018; Blümich,
 210 2019; Blümich in Bastidas and Cano, 2019). Although time consuming, high-resolution depth profiles of
 211 volumetric, quantitative moisture content are more significant than the volume-averaged numbers delivered by
 212 most methods other than the NMR-MOUSE including evanescent field dielectrometry (Olmi et al., 2006). The
 213 latter method derives moisture content and the presence of salt from the dielectric properties of a wall exposed to
 214 an electric field with a frequency of about 1 GHz. The electric wave enters the wall up to about 20 mm, so that the
 215 delivered moisture content is a weighted volume average across that depth range. While the measurement is fast,
 216 the depth resolution is inadequate for further analysis, because the moisture content varies significantly over the
 217 20 mm as demonstrated with measurements of wall moisture in the Chapel of St. Mary of the Abbaye de Chaalis
 218 (Fig. 4). Volumetric moisture content is easy to quantify at short echo time, by simply taking the signal amplitude
 219 from a particular spot inside the wall and normalizing it to the amplitude of the signal from pure water measured
 220 with the same instrumental parameter settings.
 221

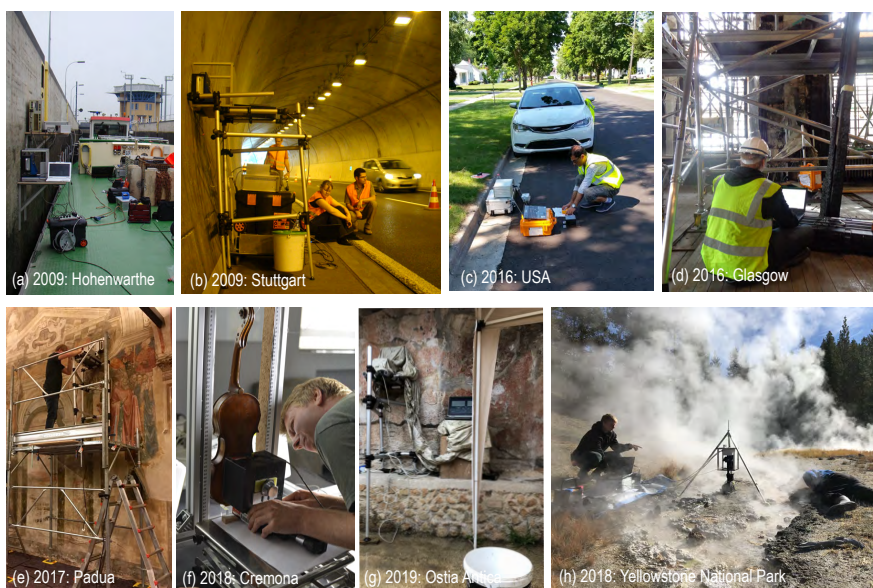


222
 223 Figure 4. Moisture measurements at the painted wall left of the altar inside the Chapel of St. Mary in Chaalis. a)
 224 Set-up for NMR depth profiling. b) High-resolution depth profiles from eight positions. The moisture-content
 225 values from evanescent field dielectrometry (EFD) are compared to NMR values derived from integration of
 226 quantitative moisture depth profiles weighted with the heuristic depth attenuation function, which is indicated by
 227 the shaded region in the bottom left profile.
 228

229 The measurement conditions encountered in historic buildings and outdoors are often challenging to meet
 230 with equipment designed for laboratory use (Fig. 5). Examples are the presence of water, rain or steam (Fig.
 231 5a,g,h), passing cars (Fig. 5b,c), testing spots a few meters high (Fig. 5d,e), and treasures of outstanding value
 232 inside a guarded museum laboratory (Fig. 5f). The climate conditions can range from hot, e.g., up to 38° C air
 233 temperature (Fig. 5c) and close to boiling water temperature (Fig. 5h) to cold, e.g. down to 5° C (Fig. 5a). The
 234 environment may be dusty with magnetic sand particles or wet from streaming rain (Fig. 5g). In many cases, a
 235 power grid can be accessed, but in some cases, the equipment needs to be operated from a battery (Fig. 6h) or an
 236 electric power generator. Apart from the power supply, different units need to be connected with several cables at

237 the site. These units are an NMR-MOUSE with 10 mm or 25 mm depth range, a precision translational stage, a
 238 fragile spectrometer console, and a laptop computer. The electrical connectors can break during transport and
 239 assembly. The connecting cables often form ground loops that produce 50/60 Hz hum and pick up environmental
 240 electromagnetic noise. However, the latter can successfully be shielded in most cases with the help of silver-coated
 241 and electrically grounded parachute silk (Fig. 5g) or rabbit fence. Moreover, a stable scaffold finely adjustable in
 242 height and suitable to be set up on uneven ground is needed to accurately position the NMR-MOUSE at the spot
 243 of interest (Fig. 4a). All these parts along with basic tools for emergency repair are usually packed into plastic
 244 transportation boxes and shipped to the site of interest prior to the measurement campaign.

245



246

247 Figure 5. The MOUSE outside the house. a) Profiling the moisture content of the grey concrete wall of the lock
 248 Hohenwarthe. b) Profiling moisture in the concrete wall of the Gäubahn tunnel near Stuttgart. c) Analyzing the
 249 crumb-rubber content in asphalt pavement (Foto: Yadoallah Teymouri). d) Assessing the fire damage of sandstone
 250 in the Mackintosh library of Glasgow. e) Searching for a hidden Giotto fresco in Padua. f) Measuring a depth
 251 profile through the back of a Stradivari violin in Cremona. g) In search for a hidden wall painting in Ostia Antica
 252 on a rainy day. h) Profiling sediment-covered biofilms at the hot springs in Yellowstone National Park.

253

254 A practical point of concern in measuring high-resolution depth profiles is the proper placement of the
 255 sensitive slice parallel to the stratigraphy of the object. Assuming that the sensitive slice is 10 mm wide and 0.1
 256 mm thick, the misalignment angle between the plane of the slice and the layers to be resolved needs to be smaller
 257 than one degree (Blümich et al., 2020). With a laboratory setup, the sensitive slice and the object surface can be
 258 accurately aligned when the NMR-MOUSE is properly placed on the sample table of the lift to which the sensitive
 259 slice had been aligned by the manufacturer (Fig. 1a). But measurements in the field usually employ a translation
 260 stage without a sample table (Figs. 4a, 5f, 5h) so that the sensor is aligned with the object surface by eye. Moreover,
 261 the minimum distance between the sensor and the object needs to be as small as possible, i. e. 1 mm or less, at the
 262 start of profiling in order to maximize the depth range into the object. Setting alignment and minimum distance is

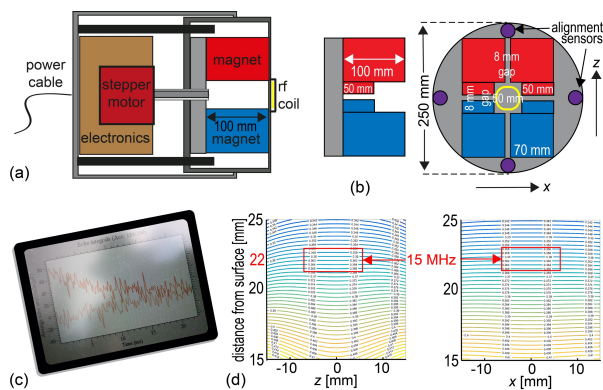
263 a critical part of the experiment setup. Electronic guidance for both would greatly simplify the setup procedure
264 and improve the reproducibility of measurement.

265 4. Improving the fitness of the NMR-MOUSE for adventures outside the house

266 It is the accumulated experience with cultural heritage studies, which suggests a number of improvements to bring
267 the NMR-MOUSE in shape for the adventures encountered when leaving the house and operating outdoors. These
268 are:

- 269 1) Combine all electronics into one instrument comprising the translation stage, the NMR-MOUSE and the
270 transmit-receive electronics.
- 271 2) Incorporate distance and alignment sensors into the instrument.
- 272 3) Employ a stable sensor scaffold and mounting device that can be assembled quickly at the site and enables
273 measurements at different heights.

274



275

276 Figure 6. Concept of an all-in-one NMR-MOUSE for depth profiling. a) Axial cross section through two telescoped
277 tubes showing the stepper motor along with the transmit-receive electronics on the left in the outer tube and the
278 NMR-MOUSE on the right in the inner tube. b) Arrangement of magnets and alignment sensors. c) The instrument
279 should be controlled via WLAN or Bluetooth. d) Calculated field map predicting the position of the sensitive slice
280 at 22 mm above the magnet surface.

281 4.1 The all-in-one instrument

282 The envisioned all-in-one NMR-MOUSE for depth profiling outdoors would have a minimum number of
283 components connected by cables (Fig. 6). The components need to be small for ease of transportation and rugged
284 for operation outdoors. The power supply would be either a 12 V car battery or a power supply that connects to
285 the grid or an electric generator. It hooks up to the NMR instruments (Fig. 6a) with the only cable of the setup.
286 The instrument comprises the translation stage, the transmit-receive electronics, and the magnet (Fig. 6b). It would
287 be operated in wireless mode via WLAN or Bluetooth from a tablet personal computer (Fig. 6c), so that it can be
288 set up on tall scaffolds (Fig. 5e), and long measurements could be controlled and monitored from the distance
289 including the hotel room at night.

290 Assuming a 250 mm inner diameter tube, a computer simulation suggests that a Profile NMR-MOUSE
291 magnet configuration would produce a sensitive slice 22 mm above the magnet surface (Fig. 6d) with a field

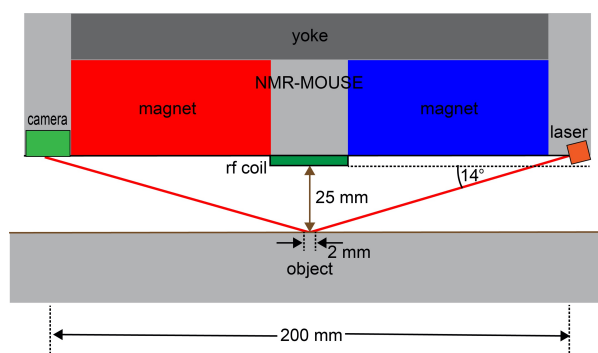
292 strength corresponding to a 15 MHz ^1H resonance frequency. Subtracting the space for the coil and the case, the
293 resultant depth of access would be 15 mm, which is a reasonable working depth for many applications ranging
294 from easel paintings to violins and frescoes. The magnets would be mounted in the inner of two telescoped tubes,
295 which can slide in and out of the outer one under control of a precision stepper motor. The outer tube would house
296 the stepper motor and the transmit-receive electronics and be attached to the mounting gear for depth profiling.
297 The total length of the pipe assembly would be shorter than 300 mm.

298 Commercial tabletop NMR instruments employ compact transmit-receive electronics (Blümich et al., 2014;
299 Blümich, 2016; Blümich and Singh, 2018), which, although reliable, nevertheless, are too large and power-hungry
300 for mobile use. Their state-of-the-art has been surpassed by the development of smaller, single-chip based
301 magnetic resonance transceivers (Zalesskiy et al., 2014; Ha et al., 2014; Ha et al., 2015; Grisi et al., 2015; Chu et
302 al., 2017; Anders et al., 2017). In particular, a small monolithic spectrometer has been developed (Bürkle et al.,
303 2020), which uses a high-voltage CMOS process with supply voltages up to 25 V for enhanced driving strength to
304 combine the monolithic NMR-on-a-chip approach with macroscopic, cm-sized coils. This approach promises a
305 90° -pulse width of 5 μs for an echo time of 20 μs at a depth of access of 10 mm, rendering high-voltage NMR-on-
306 a-chip transceivers well suited for use in a compact all-in-one NMR-MOUSE sensor.

307 4.2 Distance and alignment sensors

308 The implementation of distance and alignment sensors is a highly needed improvement over the current state-of-
309 the-art, where the NMR sensor has to be aligned visually parallel to the object as close as 0.5 mm (Blümich et al.,
310 2020). The misalignment angle of the sensitive slice with the parallel layer structures of the object needs to be less
311 than one degree if the spatial resolution is to be better than 200 μm . But visual alignment parallel to an extended
312 surface is hardly possible as one cannot see by eye the narrow gap between the magnet and the surface.
313 Nevertheless, in practice, object and sensor have usually been aligned visually (Fig. 5f,h) with surprisingly good
314 results in most cases but only fair reproducibility even for expert users. To enable the required reproducibility,
315 alignment sensors need to be incorporated with the help of which the sensitive plane can be accurately aligned
316 with the object at a fixed distance. Once aligned at a known distance, the sensor can be advanced or retracted to
317 its starting position with the stepper motor.

318



319

320 Figure 7. Concept of distance sensing with a laser beam at shallow incidence. If the alignment angle of the
321 reflecting plane changes by 0.2° , the reflected laser beam is displaced from the center of the detector camera by 4
322 mm.

323

324 Elements for alignment-sensor components can be mounted in the four spaces of the inner tube delineated
325 by the tube's inner surface and the secants defined by the outer magnet surfaces (Fig. 5b). Different sensing
326 principles can be considered. The surface spot to align the sensor with the object needs to be at least one millimeter
327 wide to average effects of surface roughness. Therefore, ultrasonic distance sensors appear to be more suitable
328 than regular laser-point distance sensors with spot widths of 10 mm vs. 70 μm , respectively. Yet commercial
329 ultrasonic sensors measure distances within a 25 mm range with 0.75 mm reproducibility, which is an order of
330 magnitude short of the required alignment accuracy if the sensors are 200 mm apart. Therefore, a better option are
331 distance sensors built from lasers with a shallow angle of incidence of 14°, which illuminate a 2 mm diameter spot
332 in the center underneath the coil at 25 mm distance from the coil surface and receive the reflected light with a
333 camera. A back-of-the-envelope calculation shows that an angle maladjustment of 0.25° will shift the center of the
334 reflected laser beam by 4 mm when laser and detector are 200 mm apart (Figs. 6, 7). This design will provide the
335 needed accuracy and precision for alignment at a fixed distance of 25 mm. Following parallel alignment of
336 sensitive slice and object surface, the gap between sensor and object can be shorted under control of the stepper
337 motor before starting the acquisition of a depth profile by retracting the sensor from the wall in defined steps
338 between measurements.

339 4.3 Operating software

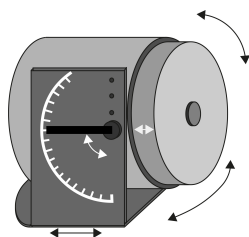
340 To operate the equipment at locations with restricted spatial access (Fig. 5e) a wireless control strategy should be
341 followed. The two most important operations to be under remote control are the control of the stepper motor and
342 the data acquisition. A depth profile is typically acquired in two runs. A first profile is acquired at low spatial
343 resolution and signal-to-noise ratio to determine the exact location and depth range of interest. Subsequently, a
344 high-resolution profile is acquired with more scans per spot and smaller step size. Depending on the required
345 information and the time available, either full multi-echo decays are measured for further analysis in terms of
346 distributions of relaxation times, or only the first points of the decays are recorded to determine proton density
347 corresponding, for example, to volumetric moisture content. The measurement progress during depth profiling is
348 usually monitored in regular intervals to catch sporadic noise interference, uninformative data, and erroneous
349 parameter settings as budgeting time is important due to up to two hours long acquisition times for a depth profile
350 and limited access time in museums, historic buildings, and at excavation sites.

351 While operating the NMR-MOUSE appears to be a simple endeavor to most people with a basic
352 understanding of NMR relaxometry or MRI (Blümich et al., 2014; Johns et al., 2016), it is a true barrier to most
353 others interested in using it for materials testing. Therefore, the operating platform should avoid NMR jargon as
354 much as possible and relate the NMR acquisition parameters to object-specific information such as hard, soft, wet,
355 moist, dry, moisture content, component concentration, duration of measurement, etc., which have to be entered
356 by the operator. Prior to measurement, the proper functioning of the equipment needs to be checked, in particular,
357 the noise-level and the phase angle of the transverse magnetization. The proper functioning of the equipment and
358 potential faults should be flagged, and the receiver phase angle be adjusted automatically if needed. Moreover, it
359 should be possible to measure again particular depth ranges identified in previous scans. All raw data need to be
360 saved for later access and processing in expert mode. In addition to the data acquisition, the operating platform
361 needs to include data processing routines, that allow to derive depth profiles with different contrast types from the
362 acquired data, e. g. hydrogen concentration (spin density), relaxation (T_2) weighted spin density (w -parameter

363 (Blümich et al., 2014)), peak integrals and peak ratios from distributions of relaxation times, as well as depth-
364 resolved distributions of relaxation times. The latter requires access to an inverse Laplace transform algorithm.
365 Finally, it should be possible to display the data from several measurements at the same scales for comparison and
366 interpretation of results.

367 4.4 Mounting device and scaffold

368 Given the dimensions of the magnets (Fig. 6a,b), the weight of the sensor is estimated to approach 40 kg. For depth
369 profiling, the device first needs to be positioned with high accuracy at 0.5 to 1 mm away from the surface of the
370 object, so that depth profiles can be scanned by retracting the sensor between scans in small, preset steps of
371 typically 0.05 to 0.25 mm. This way of scanning assures that the object is not damaged by setting a wrong depth
372 range. The mounting device has to enable manual fine adjustment of the sensor orientation following the readings
373 of the alignment sensors and allow stable positioning of the sensor at various angles with high precision for long
374 times from tens of minutes to a few hours.
375



376
377 Figure 8. Conceptual drawing of a sensor mounting device.
378

379 A simple mounting device fulfilling these criteria would consist of a U-shaped aluminum frame (Fig. 8). It
380 would have a flat, felt- or plastic-covered bottom without legs. Position and orientation would be adjusted
381 manually (arrows). To access all polar angles, the polar rotation axis would be adjustable to different values in the
382 device, and one would be able to turn the entire device upside down. To balance the sensor during depth profiling,
383 the horizontal position of the polar rotation axis would be at the average center of gravity for a 20 mm shift range.
384 The bottom plate would be extended at the back to provide a location for clamping the device to a scaffold or table.

385 For most studies outside the lab a modular scaffold had been employed (Fig. 4a), which can be assembled
386 from aluminum tubing with plastic joints in different ways to position the sliding table carrying the NMR-MOUSE
387 at different heights up to about two meters. Each of the three scaffold legs consists of two telescoped tubes so that
388 the legs are extendable via a long, threaded bolts which move the inner tubes in an out by rotating the bolt heads
389 from the top with a cordless electric drill. While this scaffold serves its purpose and is easy to transport and set up,
390 the scaffold is sensitive to vibrations and torsion. Moreover, it would be helpful to be able to adjust its height from
391 the bottom and not the top and with the sensor in place, in particular, when high positions need to be accessed.

392 5. Summary

393 Single-sided NMR relaxometry is a technique for nondestructive materials testing. Instruments like the NMR-
394 MOUSE have been developed for use in the laboratory. Applications are found in quality control and aging of

395 polymers and related materials, including PE pipes, PVC flooring, car tires, asphalt pavements, human skin, and
396 food products. The dead time of the current sensors limits the detection of rapidly decaying transverse
397 magnetization, e. g. from bound water in building materials like cement, from glass- and carbon-fiber-reinforced
398 polymer composites in windmill wings, and varnish on paintings and musical instruments. In addition to that, in
399 many cases, measurements need to be conducted at different depths or complete depth profiles need to be acquired.
400 This is the case, e.g., for moisture in walls, where NMR is one if not the only method that directly measures
401 quantitative water content without averaging over depth ranges where the moisture content significantly varies.
402 Emerging applications in cultural heritage studies demand equipment that can easily be transported, set up, and
403 operated. This equipment needs to be small and robust. The childhood and adolescence of the NMR-MOUSE
404 equipment have been reviewed and parental advice given for preparation of outdoor measurements and survival
405 outside the protected childhood home.

406 Acknowledgments

407 The magnet geometry and the field maps were calculated by Denis Jaschtschuk. The construction of a research
408 prototype of an outdoor NMR-MOUSE is funded by Deutsche Forschungsgemeinschaft, grant AN 984/24-1.

409 References

- 410 Anders, J., Handwerker, J., Ortman, M., Boero, G.: A low-power high-sensitivity single-chip receiver for, NMR
411 microscopy, *J. Magn. Reson.* 266, 41–50, 2017.
- 412 Anders, J.; Work in progress, 2020.
- 413 Anferova, S., Anferov, V., Adams, M., et al.: Construction of a NMR-MOUSE with Short Dead Time, *Concepts*
414 *Magn. Reson. B* 15, 15–25, 2002.
- 415 Angelova, L. V., Ormsby, B., Richardson, E.: Diffusion of water from a range of conservation treatment gels into
416 paint films studied by unilateral NMR: Part I: Acrylic emulsion paint, *Microchem. J.* 124, 311–320, 2016.
- 417 Armstrong-Smith, I.: A Briefcase Full of NMR, *The Analytical Scientist*, 26, 24–31, 2015.
- 418 Baias, M., Blümich, B.: Nondestructive testing of objects from cultural heritage with NMR, in: G.A. Webb,
419 *Modern Magnetic Resonance*, https://doi.org/10.1007/978-3-319-28275-6_29-1, 2017.
- 420 Balibanu, F., Hailu, K., Eymael, R., Demco, D. E., Blümich, B.: Nuclear Magnetic Resonance in inhomogeneous
421 fields, *J. Magn. Reson.* 145, 248–258, 2000.
- 422 Blümich, B., Anferov, V., Anferova, et al.: Simple NMR-MOUSE with a Bar Magnet, *Concepts Magn. Reson.:*
423 *Magn. Reson. Eng.* 15, 155–261, 2002.
- 424 Blümich, B., Baias, M., Rehorn, C., et al., Comparison of historical violins by non-destructive MRI depth profiling,
425 *Microchemical Journal* 158, 105219, 2020.
- 426 Blümich, B., Bruder, M., Guerlin, T., Prado, P.: Device for inspecting flat goods made of polymeric materials with
427 embedded textile strength supports, patent WO200079253A1, 20 June 1999.
- 428 Blümich, B., Casanova, F., Perlo, J., et al.: Noninvasive testing of art and cultural heritage by mobile NMR, *Acc.*
429 *Chem. Res.* 43, 761–770, 2010.
- 430 Blümich, B., Haber-Pohlmeier, S., Zia, W.: *Compact NMR*, de Gruyter, Berlin, 2014.
- 431 Blümich, B., Kölker, C., Casanova, F., Perlo, J., Felder, J.: Ein mobiler und offener Kernspintomograph:
432 *Kernspintomographie für Medizin und Materialforschung*, *Physik in unserer Zeit* 36, 236–242, 2005.

hat gelöscht: ¶

Feldfunktion geändert

434 Blümich, B., Perlo, J., Casanova, F.: Mobile single-sided NMR, *Prog. Nucl. Magn. Reson. Spectr.* 52, 197–269,
435 2008.

436 Blümich, B., Singh, K.: Desktop NMR and its applications from materials science to organic chemistry, *Angew.*
437 *Chem. Int. Ed. Eng.* 57, 6996–7010, 2018.

438 Blümich, B., Teymouri, Y., Clark, R.: NMR on the Road: Non-destructive Characterization of the Crumb-Rubber
439 Fraction in Asphalt, *Appl. Magn. Reson.* 50 497–509, 2019.

440 Blümich, B.: Concepts and Applications of the NMR-MOUSE, in: Bastidas, D. M., Cano, E.: *Advanced*
441 *Characterization Techniques, Diagnostic Tools and Evaluation Methods in Heritage Science*, Springer,
442 Cham, 61–79, 2019.

443 Blümich, B.: *Essential NMR for Scientists and Engineers*, 2nd ed., Springer, Cham, 2019.

444 Blümich, B.: Low-field and benchtop NMR, *J. Magn. Reson.* 306, 27–35, 2019.

445 Blümich, B.: Miniature and Tabletop Nuclear Magnetic Resonance Spectrometers, *Enc. Anal. Chem.* a9458, 1–
446 31, 2016.

447 Blümich, B.: *NMR Imaging of Materials*, Clarendon Press, Oxford, 2000.

448 Blümich, B.: The Incredible Shrinking Scanner, *Scientific American* 299, 92–98 2008.

449 Bürkle, H., Schmid, K., Klotz, T., Krapf, R., Anders, J.: A high voltage CMOS transceiver for low-field NMR
450 with a maximum output current of 1.4 A_{pp}, 2020 IEEE International Symposium on Circuits and Systems
451 (ISCAS), 10–21 Oct., 10.1109/ISCAS45731.2020.9181025, 2020.

452 Busse, F., Rehorn, C., Küppers, M., et al.: NMR relaxometry of oil paint binders, *Magn. Reson. Chem.* 58, 830–
453 839, 2020.

454 Callaghan, P. T., Eccles, C. D., Haskell, T. G., Langhorne, P. J., Seymour, J. D.: Earth's Field NMR in Antarctica:
455 A Pulsed Gradient Spin Echo NMR Study of Restricted Diffusion in Sea Ice, *J. Magn. Reson.* 133, 148–154,
456 1998.

457 Capitani, D., Di Tullio, V., Proietti, N.: Nuclear magnetic resonance to characterize and monitor cultural heritage,
458 *Prog. Nucl. Magn. Reson. Spectrosc.* 64, 29–69, 2012.

459 Capitani, D., Sobolev, A., Di Tullio, V. D., Mannina, L., Proietti, N.: Portable NMR in food analysis, *Chem. Biol.*
460 *Technol. Agric.* 4, 1–14, 2017.

461 Casanova, F., Blümich, B.: Two-dimensional imaging with a single-sided NMR probe, *J. Magn. Reson.* 163, 38–
462 45, 2003.

463 Casanova, F., Perlo, J., Blümich, B., eds.: *Single-Sided NMR*, Springer, Berlin, 2011.

464 Chu, A., Schlecker, B., Handwerker, J., et al.: VCO-based ESR-on-a-chip as a tool for low-cost, high-sensitivity
465 food quality control, IEEE Biomedical Circuits and Systems Conference (BioCAS), Turin, 1–4, 2017, doi:
466 10.1109/BIOCAS.2017.8325172, 2017.

467 Coates G. R., Xiao, L., Prammer, L. G.: *NMR Logging Principles and Applications*, Halliburton, Houston, 1999.

468 Dalitz, F., Cudaj, M., Maiwald, M., Guthausen, G.: Process and reaction monitoring by low-field NMR
469 spectroscopy, *Prog. Nucl. Magn. Reson. Spectrosc.* 60, 52–70.

470 Danieli, E., Perlo, J., Blümich, B., Casanova, F.: Small magnets for portable NMR spectrometers, *Angew. Chem.*
471 *Int. Ed.* 49, 4133–4135, 2010.

472 Eidmann, G., Savelsberg R., Blümli, P., Blümich, B.: The NMR MOUSE, a mobile universal surface explorer,
473 *J. Magn. Reson.* A122,104–109, 1996.

Feldfunktion geändert

Feldfunktion geändert

474 Fife, G. R., Stabik, B., Kelley, A. E., et al.: Characterization of aging and solvent treatments of painted surfaces
475 using single-sided NMR, *Magn. Reson. Chem.* 53, 58–63, 2015.

476 Fukushima, E.: Introduction, in: Johns, M. L., Fridjohnsson, E. O., Vogt, J. J., Haber, A., eds.: *Mobile NMR and*
477 *MRI: Developments and Applications*, Royal. Soc. Chem., Cambridge, 1–10, 2016.

478 Grisi, M., Gualco, G., Boero, G.: A Broadband Single-chip Transceiver for Multi-nuclear NMR Probes, *Rev. Sci.*
479 *Instrum.* 86, 044703, 2015.

480 Gutowsky, H. S., Meyer, L.H., McClure, R. E.: Apparatus of Nuclear magnetic Resonance, *Rev. Sci. Instrum.* 24,
481 644–652, 1953.

482 Ha, D., Paulsen, J., Sun, N., Song, Y.-Q., Ham, D.: Scalable NMR Spectroscopy with Semiconductor Chips, *Proc.*
483 *Nat. Acad. Sci.* 111, 11955–11960, 2014.

484 Ha, D., Sun, N., Ham, D.: Next-Generation Multidimensional NMR Spectrometer Based on Semiconductor
485 Technology, *eMagRes* 4, 117–126, 2015.

486 Hailu, K., Fechete, R., Demco, D. E., Blümich, B.: Segmental anisotropy in strained elastomers detected with a
487 portable NMR scanner, *Solid State Nucl. Magn. Reson.* 22, 327–343, 2002.

488 Haken, R., Blümich, B.: Anisotropy in Tendon Investigated in Vivo by a Portable NMR Scanner, the NMR-
489 MOUSE, *J. Magn. Reson.* 144, 195–199, 2000.

490 Hürlimann, M. D., Griffin, D. D.: Spin Dynamics of Car-Purcell-Meiboom-Gill-like sequences in grossly
491 inhomogeneous B_0 and B_1 fields and applications to NMR well logging, *J. Magn. Reson.* 143, 120–135,
492 2000.

493 Jackson J. A., Burnett, L. J., Harmon, J. F.: Remote (inside-out) NMR. III. Detection of nuclear magnetic
494 resonance in a remotely produced region of homogeneous magnetic field, *J. Magn. Reson.* 41, 411–421,
495 1980.

496 Johns, M. L., Fridjohnsson, E. O., Vogt, J. J., Haber, A., eds.: *Mobile NMR and MRI: Developments and*
497 *Applications*, Royal. Soc. Chem., Cambridge, 2016.

498 Kern, S., Wander, L., Meyer, K., et al.: Flexible automation with compact NMR spectroscopy for continuous
499 production of pharmaceuticals, *Anal. Bioanal. Chem.* 411, 3037–3046 (2019).

500 Keschenau, P. R., Klingel, H., Reuter, S., et al.: Evaluation of the NMR-MOUSE as a new method for continuous
501 functional monitoring of the small intestine during different perfusion states in a porcine model, *PLOS ONE*
502 0206697, 1–17, 2018.

503 Kleinberg, R. L., Jackson, J.A.: An Introduction to the History of NMR Well Logging, *Concepts Magn. Reson.*
504 13, 340–342, 2001.

505 Nordon, A., McGill, C. A., Littlejohn, D.: Process NMR spectrometry, *Analyst* 126, 260–272, 2001.

506 Oligschläger D., Lehmkuhl, S., Watzlaw, J., et al.: Miniaturized multi-coil arrays for functional planar imaging
507 with a single-sided NMR sensor, *J. Magn. Reson.* 254–18, 2015.

508 Oligschläger, D., Glöggler, S., Watzlaw, J., et al.: A Miniaturized NMR-MOUSE with a High Magnetic Field
509 Gradient (Mini-MOUSE), *Appl. Magn. Reson.* 46, 181–202, 2015.

510 Oligschläger, D., Kupferschläger, K., Poschadel, T., Watzlaw, J., Blümich, B.: Miniature mobile NMR sensors
511 for material testing and moisture-monitoring, *Diffusion Fundamentals* 22, 1–25, 2014.

512 Olmi, R., Bini, M., Ignesti, A., et al.: Diagnostics and monitoring of frescoes using evanescent-field
513 dielectrometry, *Meas. Sci. Technol.* 17, 2281–2288, 2006.

514 Perlo, J., Casanova, F., Blümich, B.: Ex situ NMR in highly homogeneous fields: ^1H spectroscopy, *Science* 315,
515 1110–1112, 2006.

516 Perlo, J., Casanova, F., Blümich, B.: Profiles with microscopic resolution by single-sided NMR, *J. Magn. Reson.*
517 176, 64–70, 2005.

518 Perlo, J., Demas, V., Casanova, F., et al.: High-resolution NMR spectroscopy with a portable single-sided sensor,
519 *Science* 308, 1229, 2005.

520 Prati, S., Sciuotto, G., Volpi, F., et al.: Cleaning oil paintings: NMR relaxometry and SPME to evaluate the effects
521 of green solvents and innovative green gels, *N. J. Chem.* 43, 8229–8238, 2019.

522 Presciutti, F., Perlo, J., Casanova, F., et al.: Noninvasive nuclear magnetic resonance profiling of painting layers,
523 *Appl. Phys. Lett.* 93, 033505, 2008.

524 Proietti, N., Capitani, D., Rossi, E., Cozzolino, S., Segre, A. L.: Unilateral NMR study of a XVI century wall
525 painted, *J. Magn. Reson.* 186, 311–318, 2007.

526 Rehorn, C., Blümich, B.: Cultural Heritage Studies with Mobile NMR, *Angew. Chem. Int. Ed. Eng.* 57, 7304–
527 7312, 2018.

528 Rehorn, C., Kehlet, C., Del Federico, E., et al.: Automatizing the comparison of NMR depth profiles, *Strain* 54,
529 e12254, 2018.

530 Rühli, F., Böni, T., Perlo, J., et al.: Non-invasive spatial tissue discrimination in ancient mummies and bones in
531 situ by portable nuclear magnetic resonance, *J. Cultural Heritage* 8, 257–263, 2007.

532 Saalwächter, K.: Microstructure and dynamics of elastomers as studied by advanced low-resolution NMR
533 methods, *Rubber Chem. Tech.* 85, 350–386, 2012.

534 Segre, A. L., Blümich, B.: Progetto 'MOUSE': Risonanza magnetica per i beni culturali, *Ricerca & Futuro* 25, 34–
535 36, 2002.

536 Van Landeghem, M., Danieli, E., Perlo, J., Blümich, B., Casanova, F.: Low-gradient single-sided NMR sensor for
537 one-shot profiling of human skin, *J. Magn. Reson.* 215, 74–84, 2012.

538 van Putte, K., van den Enden, J.: Fully automated determination of solid fat content by pulsed NMR, *J. Am. Oil*
539 *Chem. Soc.* 51 316–320, 1974.

540 Varian, R. H.: Apparatus and Method for Identifying Substances, US patent 2,651,490, filed 3 January 1952.

541 Watzlaw, J., Glöggl, S., Blümich, B., Mokwa, W., Schnakenberg, U.: Stacked planar micro coils for single-sided
542 NMR applications, *J. Magn. Reson.* 230, 176–185, 2013.

543 Woessner, D. E.: The Early Days of NMR in the Southwest, *Concepts Magn. Reson.* 13, 77–102, 2001.

544 Zaleskiy, S.S., Danieli, E., Blümich, B., Ananikov, V. P.: Miniaturization of NMR systems: desktop
545 spectrometers, microcoil spectroscopy, and "NMR on a chip" for chemistry, biochemistry, and industry,
546 *Chem. Rev.* 114, 5641–5694 (2014).